  Bull. Chem. Soc. Jpn., 61, 1—11 (1988)

Invited Paper

Is Accurate X-Ray Analysis Worthwhile?

Jack D. DUNITZ

Organic Chemistry Laboratory, Swiss Federal Institute of Technology,
ETH-Zentrum, CH-8092 Zürich, Switzerland
(Received August 3, 1987)

Following a brief introduction to X-ray analysis, three areas are discussed where accurate measurements can lead to results of interest to chemistry. These areas are: (a) molecular geometry, (b) molecular motions in the solid state, (c) experimental electron density distributions. As the technical possibilities for accurate X-ray analysis improve, important developments in all three areas can be expected.

Most chemists nowadays are aware that the last two decades or so have seen a remarkable increase in the *ease* and *rapidity* with which X-ray crystal structure analyses can be accomplished; for this is a development that has transformed the tactics and strategies of preparative chemistry, both in the organic and organometallic areas. Almost as well known is the impressive increase in the *complexity* of the structures that can be elucidated at atomic or near atomic resolution, a development which is beginning to provide the structural basis for understanding and controlling many biochemical processes, with obvious implications for biology and medicine. Less well known, perhaps, is the remarkable improvement in the *accuracy* attainable in modern X-ray structure analysis. This particular improvement is due to instrumental and computational developments but also to the increased attention that has been paid to various sources of systematic error in the diffraction experiment.[1] Another most important factor is the sheer increase in the number of available diffractometers, thanks to which it no longer necessary to make the measurements in a hurry.

In this paper I shall mention three areas where this improved accuracy can lead to results of interest in chemistry: (a) small differences in bond length can be correlated with differences in chemical reactivity; (b) anisotropic displacement parameters can provide information about molecular motions in crystals and also about internal molecular motions; (c) electron density measurements provide an experimental approach to questions of chemical bonding. Before we discuss these developments, we first require a very brief introduction to X-ray crystallography in general.[2]

X-Ray Analysis in a Nutshell

When X-rays pass through matter they are scattered by the extra-nuclear electrons. In a crystal the electron density $\rho(\boldsymbol{X})$ is periodic and can therefore be represented as a Fourier series.

$$\rho(\boldsymbol{X}) = (1/V)\Sigma|F(\boldsymbol{H})|\cos[2\pi\boldsymbol{H}\cdot\boldsymbol{X}-\alpha(\boldsymbol{H})], \quad (1)$$

where V is the volume of the unit cell. The coefficients $|F(\boldsymbol{H})|$ of this series can be shown to correspond to the amplitudes of the diffracted beams in the directions of the scattering vector $\boldsymbol{H}(h_1, h_2, h_3)$. These amplitudes can be measured in an X-ray diffraction experiment. In order to reconstruct the electron density $\rho(\boldsymbol{X})$, we also need the corresponding phase angles $\alpha(\boldsymbol{H})$, as expressed in Eq. 1, that is, we need to know whether each Fourier wave starts at the origin with a maximum ($\alpha=0$) or a minimum ($\alpha=\pi$) or some intermediate value. This is the well known "phase problem," and methods are available for solving it.[3] For centrosymmetric crystals α is limited to the values 0 or π. Since $|F(\boldsymbol{H})|$ can be measured and $\alpha(\boldsymbol{H})$ can be obtained indirectly, there is nothing to stop us from evaluating the electron density $\rho(\boldsymbol{X})$ at each point $\boldsymbol{X}(x_1, x_2, x_3)$ of the unit cell by summation of the Fourier series in Eq. 1. Since the atomic nuclei are located at the points of maximum density (or, more correctly, at the centroids of the individual density peaks), the atomic arrangement can then be read off directly from $\rho(\boldsymbol{X})$. This is the way most crystal structures are solved.

Unfortunately, the electron density obtained from Eq. 1 is not quite true. In order to build up a faithful image of $\rho(\boldsymbol{X})$ we would need an infinite number of terms in the Fourier series. With a finite number of terms, the image is flawed by what is called "termination of series error," which consists mainly of spurious, more or less spherical, ripples of electron density emanating outwards from the atomic peaks. In most modern structure analyses, the set of atomic positions derived from $\rho(\boldsymbol{X})$ serves merely as a starting point for a series of non-linear least-squares refinements. Essentially, the parameters describing the atomic arrangement are adjusted to obtain optimal agreement with measured values of $|F(\boldsymbol{H})|$. The passage from the continuous electron density function $\rho(\boldsymbol{X})$ to the parametrized discrete-atom model runs something along the following lines.

By inversion of Eq. 1 we can express the complex structure amplitudes $F(\boldsymbol{H})$ as the Fourier transform of the continuous electron density within a unit cell,

$$F(\boldsymbol{H}) = \int \rho(\boldsymbol{X}) \exp[2\pi i\boldsymbol{H}\cdot\boldsymbol{X}]\mathrm{d}\boldsymbol{X}. \quad (2)$$

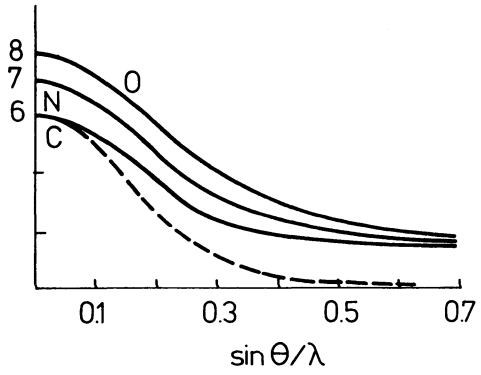

Fig. 1. Atomic scattering factors (form factors) for C, N, and O atoms at rest. The scattering factor is also shown for a C atom with mean-square displacement amplitude of 0.1 Å².

We now approximate $\rho(\boldsymbol{X})$ as a superposition of spherical density peaks associated with a set of non-interacting atoms at the positions $\boldsymbol{X}_j$ to obtain

$$\begin{aligned} F(\boldsymbol{H}) &= \int \Sigma \rho_j(\boldsymbol{X}-\boldsymbol{X}_j) \exp[2\pi i \boldsymbol{H}\cdot\boldsymbol{X}] \mathrm{d}\boldsymbol{X} \\ &= \Sigma \int \rho_j(\boldsymbol{X}-\boldsymbol{X}_j) \exp[2\pi i \boldsymbol{H}\cdot(\boldsymbol{X}-\boldsymbol{X}_j)] \\ &\qquad \times \exp[2\pi i \boldsymbol{H}\cdot\boldsymbol{X}_j] \mathrm{d}\boldsymbol{X} \\ &= \Sigma f_j(\boldsymbol{H}) \exp[2\pi i \boldsymbol{H}\cdot\boldsymbol{X}_j], \end{aligned} \tag{3}$$

where

$$f_j(\boldsymbol{H}) = \int \rho_j(\boldsymbol{X}) \exp[2\pi i \boldsymbol{H}\cdot\boldsymbol{X}] \mathrm{d}\boldsymbol{X}.$$

Since the atoms are assumed to have spherical symmetry, this integral can be written as

$$f_j(R) = 4\pi \int r^2 \rho(r) \frac{\sin 2\pi Rr}{2\pi Rr} \mathrm{d}r, \tag{4}$$

where r and R are radial distances in real and reciprocal space, respectively. The quantity $f_j(R)$ is the scattering power of the jth atom and is independent of the atomic position $\boldsymbol{X}_j$. Atomic scattering factors (form factors) for isolated neutral and ionic atoms have been calculated by many authors using various quantum mechanical models to obtain the appropriate electron densities; standard tabulations are given in International Tables for X-Ray Crystallography.[4] At zero scattering angle ($\boldsymbol{H}=0$), all electrons scatter in phase, so $f_j(0)$ equals the total number of electrons in the respective atom or ion. As the scattering angle increases ($|H|=2\sin\theta/\lambda$), interference between different regions of the electron cloud reduces the net scattering power, but even at large angles the inner core electrons are still scattering in phase (Fig. 1.)

Atomic Motion in Crystals

The atoms in a crystal are not stationary. From diffraction studies it is possible to obtain information not only about the mean atomic positions but also about the probability density functions (pdf's) of the atoms resulting from the time-averaged motion, averaged again over all unit cells in the crystal. In small molecule crystallography, the atomic pdf's are usually taken as trivariate Gaussian probability functions, except for hydrogen atoms which are taken as isotropic because their weak scattering power precludes the use of too many parameters in the description of their averaged motion. The atomic ellipsoids in the ORTEP diagrams[5] used to illustrate so many crystal structures are bounding surfaces that enclose some specific probability, usually 0.5, hence "50% probability ellipsoids." With these assumptions each atomic scattering factor has to be multiplied by the Fourier transform of the corresponding pdf, often referred to as the "anisotropic temperature factor," $T_j(\boldsymbol{H})$, which may be written in a compact form as

$$T(\boldsymbol{H}) = \exp(-2\pi^2 \boldsymbol{H}^T \boldsymbol{U} \boldsymbol{H}), \tag{5}$$

where $\boldsymbol{U}$ is a symmetric matrix, the matrix of second moments of the pdf. The second moment of the pdf in a given direction defined by a unit vector $\boldsymbol{n}$, i.e. the mean-square displacement of the atom in that direction, is then $\boldsymbol{n}^T\boldsymbol{U}\boldsymbol{n}$. The six components of $\boldsymbol{U}$ (or only one in the isotropic case) for each atom are included (as anisotropic displacement parameters or ADP's, together with the usual atomic positional parameters) in the least-squares analysis. In principle, higher cumulants of non-Gaussian pdf's can also be determined — 10 cubic terms, 15 quartic, and so on — but there are difficulties. The main problem is that these higher terms are only likely to be important when the second moments of the atomic pdf's are very large; however, the larger the second moments, the more rapidly the scattering from the atomic centre in question falls off with scattering angle. Thus, it is just when the higher terms become important that they become virtually impossible to measure.

Accuracy in Atomic Positions from X-Ray Diffraction

Atomic positions determined by X-ray diffraction correspond to centroids of distributions obtained by convoluting the atomic charge distributions with the corresponding pdf's. For small to medium sized molecules, these centroids are obtainable with nominal standard deviations of the order of a few thousandths of an Å, an uncertainty range that is usually considerably smaller than the built-in uncertainties involved in the derivation of averaged molecular structural parameters in systems where the

atoms are undergoing vibration. Since the relative phases of the vibrating atoms are generally unknown, separations between atomic centroids cannot be interpreted directly as interatomic distances.[6] The larger the mean-square displacements, the larger the uncertainties. In addition, atomic positions from X-ray analyses of molecular crystals based on low-angle[7] diffraction data are prone to systematic errors arising from asphericity in the distribution of the valency electrons. These errors can be reduced somewhat by appropriate weighting of the observations in the least-squares analysis.[8] However, it is much better to cool the crystals as far as possible to reduce the vibrational motion and try to measure the diffracted intensity at higher scattering angles. Atomic positions obtained from least-squares refinement of sufficiently extensive high-angle, low-temperature X-ray data can be expected to correspond closely to nuclear positions (as obtained from neutron diffraction data) and should be relatively free from systematic error. Indeed, for a small molecule, 2-aminopropenenitrile, atomic positions from 97 K X-ray diffraction data yield rotational constants very close to those obtained from a microwave spectroscopic study of the molecule in the gas phase.[9]

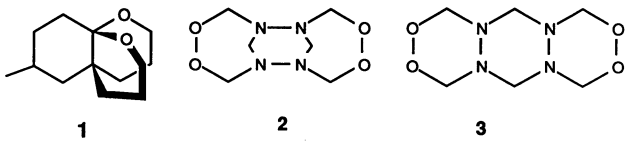

1 2 3

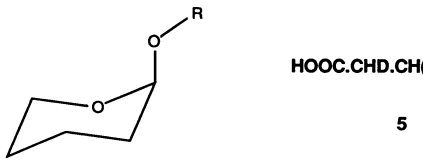

4

HOOC.CHD.CH(OH).COOH

5

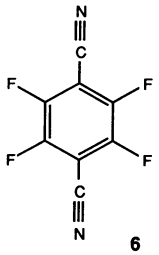

6

Accurate X-ray analysis can reveal subtle structural expressions of stereo-electronic effects.[10] In the dioxapropellane ketal **1** the two oxygen atoms O5 and O14 are chemically similar[11] but conformationally different (Fig. 2). From a crystal structure analysis at 98 K[12] the only pair of chemically equivalent bonds that shows an appreciable (>0.003 Å) difference in bond length is C6—O5, 1.412 Å, and C6–O14, 1.438 Å, difference 0.026 Å, with estimated standard deviation (esd) less than 0.003 Å. As seen in Fig. 2, the longer bond C6–O14 is synclinal (*sc*) to O5–C4 and hence antiperiplanar (*ap*) to a tetrahedral lone pair on O5, whereas the shorter bond C6—O5 is *ap* to O14—C13. The observed difference of 0.026 Å is in pleasing agreement with results of calculations on methanediol and methoxymethanol in the *sc,ap* conformation, which predict a relative lengthening by 0.025—0.030 Å of the C–O bond *ap* to a lone pair.[13]

Very similar results are observed for the tetraaza-tetraoxa-tricyclic molecule **2** from a crystal structure analysis at 96 K.[14] From the stereoview of the molecular conformation in Fig. 3, it is seen that the molecule as a whole is centrosymmetric and that the two sides of each seven-membered ring are conformationally different. The exocyclic N1–C1 bond is 0.025 Å shorter than N2–C2, while C1–O1 is 0.017 Å longer than C2–O2, differences that again clearly depend on stereoelectronic factors, the lone pair at N1 being *ap* to the C1–O1 bond while the lone pair at N2 is anticlinal (*ac*) to C2–O2. It is interesting that **2** must be thermodynamically more stable than the isomeric structure **3**, with which the compound was previously identified.[15] In the seven-membered ring the torsion angle about the O–O bond is 100°, close to the value in hydrogen peroxide.[16] In a six-membered ring, however, with normal bond lengths and approximately tetrahedral bond angles, it is impossible to obtain a torsion angle much greater than about 60°.

Bond-length differences of the magnitude we have been discussing may be associated with significant

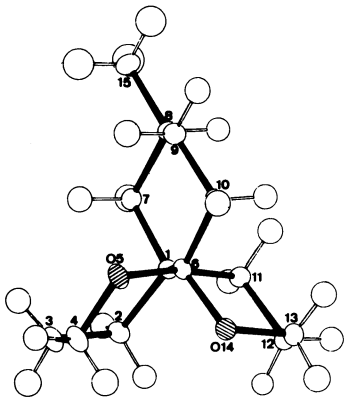

Fig. 2. View of molecule **1** at 98 K down the central C–C bond and showing atom numbering.[12]

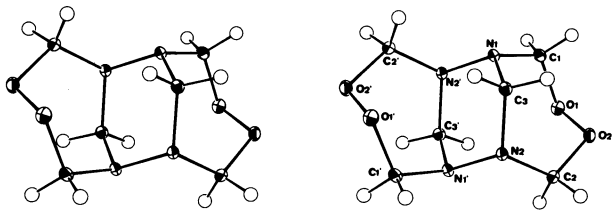

Fig. 3. Stereoview of molecule **2** at 96 K showing 50% probability ellipsoids and atomic numbering.[14]

changes in chemical reactivity. By combining crystallographic and kinetic data for acetals and related molecules, Kirby and Jones[17] found a linear relationship between the extension of a C–O bond (relative to some standard bond length) and the free energy of activation for heterolytic fission of the bond. For these reactions, and also for others,[18] it would appear that differences in the transition state are unimportant compared with differences in ground state structure. For axial aryl tetrahydropyranyl acetals **4** and for phosphate monoester anions $(ROPO_3)^{2-}$ the slope $\delta\Delta G^{\ddagger}/\delta r$ was found to be about 250 kcal mol^{-1} Å^{-1}. Thus, an increase of 0.02 Å in equilibrium bond length would correspond to a decrease of 5 kcal mol^{-1} in activation energy or to a 4000-fold increase in rate at room temperature. This astonishingly sharp sensitivity of activation energy of bond-breaking processes to quite small changes in ground-state structure can be accounted for in terms of a model involving a simple modification of the Morse equation, which is known to provide a good approximation to the potential energy of many classes of bonds.[19]

These results underline the need for accurate bond length measurements in structural studies bearing on questions of chemical reactivity.

Accuracy of Atomic Displacement Parameters from X-Ray Diffraction

Atomic displacement parameters (U values or ADP's) are calculated for thousands of crystal structure analyses each year, but the results do not seem to be generally regarded as being of any particular interest, at any rate not interesting enough to justify their publication in scientific journals. In fact, ADP's have practically disappeared from the published literature.[20] While one can sympathize with the reluctance of Journal Editors to publish long lists of numbers (six per atom for the usual Gaussian ADP's), the virtual disappearance of these data seems a pity because ADP's from reasonably careful routine analyses based on modern diffractometer measurements may often yield physically significant information about the atomic motions. Indeed, there is an ironical twist to the circumstance that most ADP's to be found in the literature are of poor quality. The reason for this is that just about the time when routine analyses were beginning to produce reasonably reliable numbers for these quantities, Editorial Boards were deciding against them. For the last few years ADP's have mostly been relegated to the category of supplementary information to be deposited and filed away in the vaults of scientific societies, publishing houses, libraries and similar depositaries.[21]

In the meantime, however, several studies have shown that ADP's from diffraction studies can yield important information not only about the molecular rigid-body motion but also about the internal molecular motion and other dynamical processes in crystals.[22] It is clear that for every pair of atoms A,B in a perfectly rigid grouping the mean-square displacements of both atoms must be exactly equal along the interatomic direction;

$$\Delta(\mathrm{A,B}) = \boldsymbol{n}^T\boldsymbol{U}_A\boldsymbol{n} - \boldsymbol{n}^T\boldsymbol{U}_B\boldsymbol{n} = 0, \qquad (6)$$

where $\boldsymbol{n}$ is the unit vector in the A,B direction. This condition is in effect a definition of rigidity, and if it is not satisfied within experimental accuracy there must be a relative motion of the atoms in the A,B direction. Note that the converse does not hold; Δ(A,B) may be zero if the relative motion of the atoms is perpendicular to the A,B direction. Thus, for example, the Δ values will not deviate significantly from zero for the out-of-plane vibrations of a planar molecule. Subject to this reservation, Eq. 6 provides a simple method of testing whether or not the ADP's obtained for a given molecule or molecular fragment are compatible with rigid-body behaviour.[23] Since bond-stretching vibrations typically have negligible amplitudes compared with other internal motions,[24] Eq. 6 should be valid for bonded pairs of atoms even in non-rigid molecules. Thus, evaluation of Δ(A,B) over all bonded pairs of atoms provides a useful estimate of the overall quality of the ADP's.[25] Failures of the rigid-bond criterion in certain structures have been used as a diagnostic to detect disorder among similarly shaped molecules with different bond lengths for corresponding bonds, e.g. different orientations of Jahn–Teller distorted complexes, and different spin-states of otherwise similar molecules.[26]

A visual impression of internal molecular motions can sometimes be gained simply from looking at ORTEP diagrams. Inspection of the matrix of Δ(A,B) values can reveal relative motion of rigid subgroups more objectively. Within the subgroups the Δ values should not differ significantly from zero, while relative motion of the subgroups will be manifested by much larger values of some of the inter-group Δ's. An example is given in Table 1, where Δ values for triphenylphosphine oxide in its orthorhombic crystal modification at 100 K[27] are shown. The triangles labelled A,B,C contain Δ values for the three phenyl groups (Fig. 4); the three blocks AB, AC, BC contain Δ values for pairs of atoms belonging to different rings. The esd's of the Δ's are about 7 units (Å$^2\times10^{-4}$) and the root-mean-square (rms) Δ's for the three individual rings are 11, 6, and 8 units respectively. Thus, the rings can be regarded as being essentially rigid. On the other hand, there is clear evidence of significant motion of the rings relative to one another, especially of ring A relative to rings B and C; the rms Δ values for blocks AB and AC are four or five times as large as those within the rings.

Two main methods for estimating amplitudes of

internal motion of non-rigid molecules, superimposed on the overall molecular motion,[28] have been proposed: (1) the segmented-body model, involving a network of coupled rigid bodies;[29] (2) addition of contributions from specified internal librations to those from rigid-body motion.[30] Although problems arise in connection with the correlations among internal and overall molecular librations,[31] mean-square amplitudes for torsional vibrations about bonds can be estimated reasonably well, especially when they are large compared with the overall molecular librations, and from this information (plus a knowledge of the crystal temperature) quadratic force constants for the motions in question can be derived.[32] A survey of ADP's from more than 125 crystal structures has shown that force constants estimated in this way for various librating groups are at least in the same range as those obtained by other techniques.[33]

Provided one is prepared to make a guess about the shape of the potential barrier hindering rotation of assumedly rigid groups, barrier heights can also be estimated from a knowledge of the mean-square libration amplitude $\langle\phi^2\rangle$ and the crystal temperature.

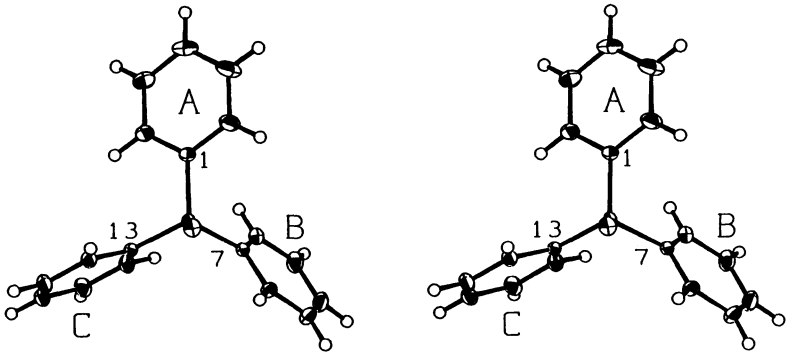

Fig. 4. Stereoview of triphenylphosphine oxide (orthorhombic modification)[27] at 100 K showing ring labels and atoms numbered 1, 7, and 13.

Table 1. Matrix of Δ values (in units of 10^{-4} Å^2) for triphenylphosphine oxide at 100 K. Each Δ is the mean-square displacement amplitude (MSDA) of the atom at the head of the column minus the MSDA for the atom at the left of the row, both MSDA's being taken along the interatomic vector. Atoms C1–C6 comprise ring A, C7–C12 ring B, C13–C18 ring C (see Fig. 4).

ATOM	C18	C17	C16	C15	C14	C13	C12	C11	C10	C9	C8	C7	C6	C5	C4	C3	C2	C1	P1
O1	0	−8	−15	−6	−6	−19	18	8	10	35	32	9	2	−15	−22	9	48	−10	−20
P1	33	31	23	25	31	10	38	32	22	31	35	22	29	25	16	24	41	13	
C1	48	28	−2	−11	−5	−9	40	44	11	−5	−3	0	11	5	5	10	21		
C2	15	5	−23	−44	−46	−34	−73	−89	−100	−77	−57	−61	−2	−7	5	−6			
C3	49	26	−22	−45	−38	−20	−21	−31	−74	−78	−57	−42	−11	−22	2				
C4	56	12	−53	−59	−34	−25	36	67	12	−31	−29	−15	−10	−16					
C5	14	−32	−78	−68	−41	−47	−25	2	−25	−40	−29	−33	−11						
C6	17	−10	−34	−32	−18	−30	−50	−34	−51	−49	−32	−44							
C7	35	42	23	20	19	3	2	−1	0	1	−6								
C8	19	13	−19	−23	−23	−36	8	−9	−9	1									
C9	19	12	−27	−32	−30	−36	5	−5	−3										
C10	27	44	13	4	−1	−12	−5	−8											
C11	−2	21	1	−3	−5	−17	−7												
C12	6	24	4	−1	−1	−11													
C13	7	16	13	7	3														
C14	0	5	7	2															
C15	−8	−13	−11																
C16	2	4																	
C17	−5																		

A

B

C

For example, rotation barriers estimated from ADP analysis for the cyclopentadienyl rings in crystalline metallocenes with the assumption of a fivefold sinusoidal potential agree well with those derived by solid-state NMR and other spectroscopic methods.[34]

Further developments in this direction could well lead during the next decade or so to an intrusion by crystallographers into the study of low-energy, large-amplitude molecular motions, a field that has traditionally been regarded as a preserve of molecular spectroscopy and gas-phase electron diffraction.

One possible use of accurate displacement parameters is to distinguish protium from deuterium in specifically labelled molecules by X-ray diffraction. This is no problem as far as neutron diffraction is concerned, since the neutron scattering powers of the two nuclei are very different, but neutron diffraction facilities are by no means so widely available. The problem with the distinction by means of X-rays is that the X-ray scattering powers of the two kinds of atom are identical. However, the heavier isotope is associated with a smaller vibrational amplitude. For a -CHD- methylene group, the difference between isotropic U_H and U_D can be estimated to be about 0.0035 Å^2, roughly double the standard deviation attainable today from low-temperature (liquid nitrogen) X-ray data of the highest quality.[35] In a practical test, it was possible to establish the relative configuration of the two stereogenic centres in deuterium-labelled malic acid **5** obtained by enzymatic addition of D_2O to fumaric acid.[36] The experiment was actually made with the crystalline mono ammonium salt and gave the same configuration as that established by neutron diffraction of the corresponding phenylethylammonium salt.[37] While it is clear that the X-ray method cannot possibly compete with neutron diffraction as far as isotope discrimination is concerned, its potentialities in this respect should not be altogether dismissed.

Another area where analysis of ADP's might be important includes studies of the nature and mechanism of phase changes, especially those involving order/disorder transformations. In ferrocene, for example, the cyclopentadienyl rings in the monoclinic high-temperature crystal modification are orientationally disordered down to the phase transition at 164 K.[38] Below this temperature the structure becomes triclinic, and the rings librate about well defined equilibrium orientations.[39]

Electron Density Maps

Electron density maps have been used for years to give images of molecules in crystals, and it has always been realized that such maps might also tell us something about the fundamental problem of the nature of the chemical bond. If only we could make those maps accurate enough they might help to illuminate for us the problem of how atoms are held together in molecules and crystals.

It was fortunate for the development of crystal structure analysis that the electron density in a molecular or ionic crystal is very closely similar to the superposition of the densities of the separated atoms, placed at the positions they occupy in the crystal. This similarity made it possible to use standard, spherically symmetric scattering factors (as expressed in Eq. 4 and Fig. 1) in solving crystal structures and also in refining them by least-squares methods. In fact, when crystallographers take pride in their low R factors,[40] they pay tribute to the goodness of the pro-crystal approximation as well as to the accuracy of their measurements. The difference $\Delta\rho(\boldsymbol{X})=\rho(\boldsymbol{X})-\rho_M(\boldsymbol{X})$ between the actual density and the pro-molecule density is known as the deformation density. It can be interpreted as representing the reorganization in the electron density that occurs when a collection of independent, isolated, spherically averaged atoms is combined to form a molecule in a crystal. Since $\Delta\rho$ is only a very small fraction of ρ in the region of the atoms, it is very susceptible to experimental error in the X-ray measurements and to inadequacies in the model (errors in the assumed atomic positions and ADP's).

The deformation density $\Delta\rho$ is conveniently obtained as:

$$\Delta\rho(\boldsymbol{X}) = (1/V)\sum\{|F(\boldsymbol{H})| - |F_M(\boldsymbol{H})|\} \times\cos[2\pi\boldsymbol{H}\cdot\boldsymbol{X}-\alpha_M(\boldsymbol{H})], \quad (7)$$

by analogy with Eq. 1, where $F_M(\boldsymbol{H})$ is calculated for the pro-crystal according to Eq. 3, suitably modified to allow for the atomic temperature factors (Eq. 5). The positions $\boldsymbol{X}_j$ and corresponding $\boldsymbol{U}_j$ components of the atoms in the pro-molecule (or pro-crystal) need to be estimated as accurately as possible by least-squares analysis, preferably using high-angle, low-temperature data, as described earlier in this article, or in a separate neutron-diffraction experiment.[41] Since the observed density $\rho(\boldsymbol{X})$ and the pro-molecule density $\rho_M(\boldsymbol{X})$ are both smeared by the vibrational motion of the atoms, so is the difference density obtained by subtracting one from the other.

In an alternative procedure, the deformation density is expressed in parametric form as the sum of a number of suitably designed functions, usually chosen as a set of multipoles, each multiplied by a radial function and centred at an atomic position. The Fourier transforms of the deformation functions are then added to the free-atom form factors with variable coefficients, which are refined, together with the atomic coordinates and ADP's, by least-squares analysis. The deformation density obtained in this way is, of course, restricted by the particular choice of deformation functions included in the model. Gen-

erally, it looks smoother than the difference density. The deformation density calculated with the multipole model is often called the static deformation density[42] since it represents the charge density reorganization in going from the vibrationless promolecule to the vibrationless molecule. This makes it more suitable for direct comparison with deformation densities obtained by quantum-mechanical calculations.

As recently discussed by Seiler,[1] it is becoming increasingly clear that dependable deformation densities require an expenditure in experimental time and effort far in excess of that involved in routine X-ray analysis. If the parameters describing the promolecule are to be obtained from X-ray data, accurate and extensive measurements of high-order reflections are required. To obtain such data, the atomic vibrations must be reduced as far as possible. It is therefore advisable to carry out the diffraction measurements with the crystal held at liquid nitrogen temperature or lower. And finally, even when all these conditions are fulfilled, the significant features of the deformation density are only a small fraction of the total density. We can maximize this ratio by dealing with light-atom structures. Indeed, until we understand how to obtain physically meaningful and interpretable maps for light-atom structures, it seems prudent to avoid crystals containing heavy elements as far as possible.

We mention here two examples of recent deformation density studies which have led to results of some chemical interest. The first example concerns tetrafluoroterephthalonitrile **6**. The molecule occupies a site of C_{2h} symmetry in the crystal, so that the asymmetric unit consists of only two atoms (C and F) in general positions plus three atoms (two C and one N) on a crystallographic mirror plane. For the deformation density study,[43] the intensities of *all* reflections within a limiting sphere of radius $\sin\theta/\lambda=1.15$ Å^{-1} were measured with Mo $K\alpha$ radiation at 98 K; most reflections were measured in all symmetry-equivalent orientations, leading to a total of 17740 measurements. After averaging equivalent reflections, 2387 independent observations were left, nearly 700 per atom in the asymmetric unit. The difference map in the molecular plane, calculated with 1269 reflections with $F>20\sigma(F)$ is shown in Fig. 5. Prominent peaks occur close to the mid-points of the ring C–C bonds ($\approx$0.6 e Å^{-3}), of the exocyclic C–C bond ($\approx$0.4 e Å^{-3}), and of the C≡N triple bond ($\approx$0.75 e Å^{-3}), as well as in a region that is clearly associated with the *sp* lone pair of the N atom ($\approx$0.25 e Å^{-3}).[44] In contrast, the difference density along the polar C–F bond does not exceed 0.1 e Å^{-3}. Difference maps calculated with slightly different atomic form factors or with pro-crystal models obtained by varying details of the least-squares refinement were not significantly different from that shown in Fig. 5.

The static deformation density map calculated on the basis of the same experimental data is shown in Fig. 6A.[45] Compared with Fig. 5, the density peaks are of slightly different shapes and heights, but, allowing for the differences in the underlying assumptions, the main qualitative features of the two maps are remarkably similar.[46] There is also a close agreement between the experimental deformation

Fig. 5. Tetrafluoroterephthalonitrile. Electron density difference map $\Delta\rho$ in the molecular plane. Contour interval 0.075 e Å^{-3}, zero and negative contours broken.[43]

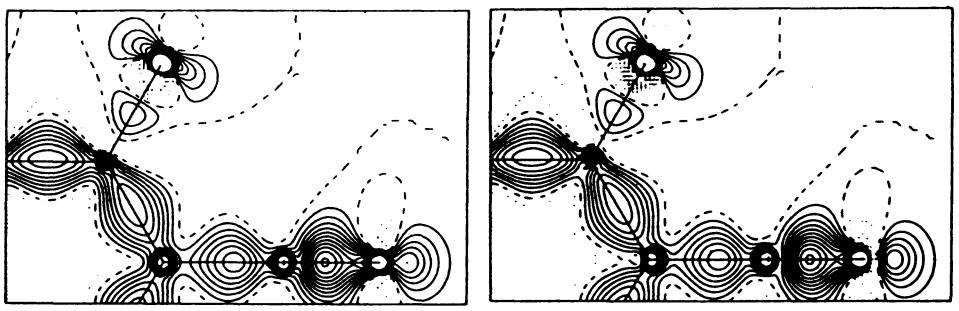

Fig. 6. Tetrafluoroterephthalonitrile. Static deformation density map in the molecular plane from (A) unconstrained, and (B) Hellmann–Feynman constrained refinements.[48] Contour interval 0.1 e Å^{-3}.

density and that calculated by density functional theory,[47] the main differences being in the lone-pair densities, which are somewhat smaller in the experimental map.

The Hellmann–Feynman theorem states that if the correct charge density is available, the forces on the atomic nuclei can be calculated by classical electrostatics; for a stable atomic arrangement, these forces must be zero. Hirshfeld has shown[48] that this condition is not fulfilled for the static deformation density shown in Fig. 6A. In particular, the electric field at the F nucleus was found to be strongly repulsive. The condition of zero net-force was then included as a constraint in the least-squares refinement with the same set of multipole terms, leading to the deformation map shown in Fig. 6B. At a first glance, the two maps look almost identical, and it may seem remarkable that one corresponds to appreciable forces on the atomic nuclei, the other to electrostatic equilibrium. The main difference is that sharp dipoles (core polarization) are produced at the nuclei, coupled with very small changes (less than 0.001 Å) in the atomic positions. Clearly, the electric field at the nuclear positions is extremely sensitive to features of the static deformation density close to the nuclei, features that are not easily determined from the X-ray data alone. The problem here is not so much the quality of the data as the strong correlation between the core polarization functions and the atomic coordinates.

For peroxides, difference maps show a density deficit at the mid-point of the O–O bond.[49,50] For example, Fig. 7 shows the difference density along the O–O bond in molecule **2**. The negative density along the bond axis contrasts with the positive density peaks corresponding to other bonding features seen in the Figure, such as the C–O and C–H bonds, as well as the O lone pairs.

In fact, from these and other studies, experimental "bonding density" seems to decrease in the order C–C>C–N>C–O≈N–N>C–F≈N–O>O–O, i.e., with increase in the number of valency electrons. This trend can be explained by comparing the tetrahedrally hybridized orbital occupation numbers for the bonded atoms with those of the spherically averaged atoms that are subtracted out.[51] It is also clear that the choice of reference states is to some extent arbitrary and that other kinds of trend could be produced by assuming non-spherical charge distributions for the atoms in the pro-molecule. Nevertheless, it may seem disturbing that the deformation-density results seem to contradict (or at least modify) the conventional wisdom about the nature of the chemical bond, namely that a build up of charge between the nuclei is necessary.[52,53] Indeed, the use of spherically averaged atoms to define the pro-molecule has come in for considerable criticism from theoreticians.[54,55] Difference densities more in line with theoretical views of chemical bonding could certainly be obtained by subtracting out suitably oriented ground-state or valence-state atoms, although such a procedure is also not without its difficulties. The choice of the reference state is clearly to some extent arbitrary. It can hardly be denied, however, that the spherically averaged density is the only choice that allows fully for the reduction in symmetry that occurs when a free atom becomes part of a molecule.

Our final example concerns the question: are ionic solids really built from ions? As Slater pointed out many years ago, the difference in charge distribution between the superposition of neutral atoms and the superposition of ions is "small and subtle, and difficult to determine by examination of the total density."[56] The main problem is that the difference between the charge densities of individual neutral atoms and corresponding ions only become appreci-

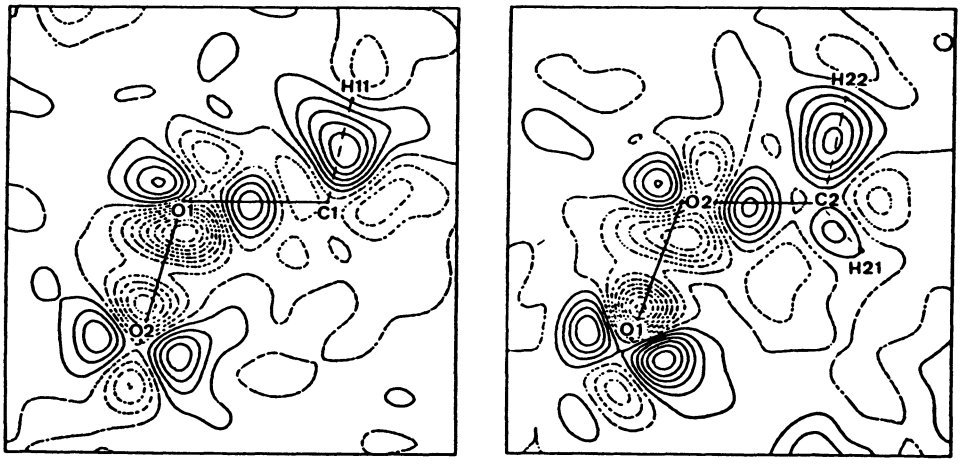

Fig. 7. Electron density difference maps $\Delta\rho$ in sections passing through the C–O–O planes of molecule **3**. Contour interval 0.075 e Å^{-3}, zero and negative contours broken.[50]

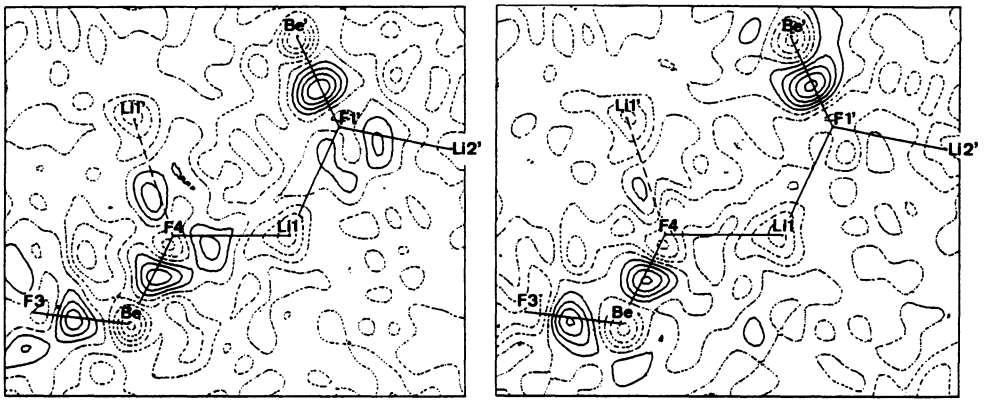

Fig. 8. Electron density difference maps $\Delta\rho$ for a chain of atoms in the Li_2BeF_4 crystal structure, based on the neutral-atom pro-crystal (left) and the ionic one (right). Contour interval 0.045 e Å^{-3}, zero and negative contours broken.[57]

able at large distances from the respective nuclei. In a crystal, where densities of neighbouring atoms overlap, this diffuse difference density cannot be unequivocally assigned to one atom or another. At these large distances, even if the density associated with a given atom may be quite small, the contribution of the spherical shell to the integrated charge may be considerable. The problem can also be expressed in terms of the respective form factors: the scattering powers (Eq. 4) of neutral atoms and of their corresponding ions differ appreciably only in a small region of reciprocal space close to the origin.

Indeed, in a new, accurate analysis of lithium tetrafluoroberyllate, Li_2BeF_4, at 81 K, both models yielded almost identical R factors[40] of 0.015 for all 6345 independent reflections out to $\sin\theta/\lambda$=1.35 Å^{-1}, an indication that the charge distribution is almost equally compatible with a superposition of neutral atom charge distributions and a superposition of ionic charges.[57] The two distributions are so similar that they can hardly be distinguished by examining the corresponding difference densities, shown in Fig. 8. Both maps show peaks of up to 0.2 e Å^{-3} along the Be–F bonds of the tetrahedral BeF_4 "anions" and still weaker ones along the Li–F directions.

Since the form factors of the neutral and ionic species differ only in the low-angle region, the intensities of the low-order reflections were re-measured in a separate experiment with a smaller crystal and with particular attention to the avoidance of systematic errors. When attention is focussed on 22 weak reflections in the region ($\sin\theta/\lambda$<0.25 Å^{-1}) where the form factors still show detectable differences, the neutral atom model reproduces the observed intensities better than the ionic one. This indicates that the diffuse charge density far from the nuclei is better represented by the superposition of outer tails of spherical distributions centred at the Li and Be atoms than by the tails of F-centred distributions.

However, since the charge distribution of the ionic model is so very similar to that of the neutral atom model, the two distributions must correspond to very similar energies. Thus, the cohesive energy estimated for an ionic model with integral charges will still be close to the correct result — and much simpler to calculate — even if the actual charge distribution happens to be slightly closer to that of the neutral atom model.[58] The fact that it is easier to calculate many properties of solids with integral point charges than with atomic charge distributions certainly makes the ionic model more convenient, but it does not necessarily make it more correct.

This work has been supported over the years by the Swiss National Foundation for Scientific Research. It has been made possible only through the dedicated collaboration of many students and colleagues, whose names are mentioned in the text and footnotes.

References

1) P. Seiler, *Chimia*, **41**, 104 (1987).
2) For a more extensive treatment along similar lines, see J. D. Dunitz, "X-Ray Analysis and the Structure of Organic Molecules," Cornell, Ithaca NY (1979).
3) J. Karle, *Science*, **232**, 837 (1986); H. Hauptman, *ibid.*, **233**, 178 (1986).
4) "International Tables for X-Ray Crystallography," Kynoch Press, Birmingham (1974), Vol. IV.
5) C. K. Johnson, ORTEP II: A Fortran Thermal-Ellipsoid Plot Program for Crystal Structure Illustrations. Report ORNL-5138, Oak Ridge National Laboratory, Oak Ridge TE (1976).
6) W. R. Busing and H. A. Levy, *Acta Crystallogr.*, **17**, 142 (1964).
7) In this context, low-angle means roughly within the limit of Cu $K\alpha$ radiation, say $\sin\theta/\lambda$ less than 0.65 Å^{-1}.
8) J. D. Dunitz and P. Seiler, *Acta Crystallogr., Sect. B*, **29**, 589 (1973).
9) P. Seiler and J. D. Dunitz, *Helv. Chim. Acta*, **68**, 2093 (1985).
10) P. Deslongchamps, "Stereoelectronic Effects in Or-

ganic Chemistry," Pergamon, Oxford (1983); A. J. Kirby, "The Anomeric Effect and Related Stereoelectronic Effects at Oxygen," Springer, Berlin (1983).

11) They would be equivalent but for their relationship to the methyl group in the third ring.

12) K. L. Brown, G. L. Down, J. D. Dunitz, and P. Seiler, *Acta Crystallogr., Sect. B*, **38**, 1241 (1982).

13) G. A. Jeffrey, J. A. Pople, and L. Radom, *Carbohydr. Res.*, **38**, 81 (1974); J. M. Lehn, G. Wipff, and H. B. Bürgi, *Helv. Chim. Acta*, **57**, 493 (1974); J. O. Williams, J. N. Scarsdale, L. Schäfer, and H. J. Geise, *J. Mol. Struct.*, **76**, 11 (1981).

14) S. N. Whittleton, P. Seiler, and J. D. Dunitz, *Helv. Chim. Acta*, **64**, 2614 (1981).

15) A. R. Katritzky, V. J. Barker, F. M. S. Brito-Palma, J. M. Sullivan, and R. B. Finzel, *J. Chem. Soc., Perkin Trans. 2*, **1979**, 1133.

16) R. M. Hunt, R. A. Leacock, C. W. Peters and K. T. Hecht, *J. Chem. Phys.*, **42**, 1931 (1965).

17) A. J. Kirby and P. G. Jones, *J. Am. Chem. Soc.*, **106**, 6207 (1984).

18) For example, hydrolysis of $[Ni(en)_n(H_2O)_{6-2n}]^{2+}$ and $[Ni(tach)_m(H_2O)_{6-3m}]^{2+}$ complexes (en=ethylenediamine, n= 0,1,2,3; tach=*cis,cis*-1,3,5-triaminocyclohexane, m=0,1,2) leads to analogous linear relationships $\delta\Delta G^*/\delta r \approx 60$ kcal mol^{-1} Å^{-1} for the rate-determining bond rupture and $\delta\Delta G^*/\delta r \approx 40$—50 kcal mol^{-1} Å^{-1} for the water-exchange reaction. G. Schwarzenbach, H. B. Bürgi, W. P. Jensen, G. A. Lawrence, L. Monsted, and A. M. Sargeson, *Inorg. Chem.*, **22**, 4029 (1983).

19) H. B. Bürgi and J. D. Dunitz, *J. Am. Chem. Soc.*, **109**, 2924 (1987).

20) Acta Crystallographica is no exception.

21) From which they can in principle be retrieved, but often only at the cost of considerable delay, inconvenience, and expense. The main problem is that supplementary data that are not printed are rarely checked. As a result, deposited ADP's, when they can be found at all, are riddled with errors that are difficult to detect and sometimes impossible to correct. Some journals lack a deposition scheme altogether, so that data supplementary to papers published in them are simply lost.

22) For a recent, more detailed account of the potentialities and limitations of interpreting ADP's, see J. D. Dunitz, V. Schomaker, and K. N. Trueblood, *J. Phys. Chem.* in press.

23) R. E. Rosenfield, K. N. Trueblood, and J. D. Dunitz, *Acta Crystallogr., Sect. A*, **34**, 828 (1978).

24) Except where the masses of the atoms involved differ greatly.

25) F. L. Hirshfeld, *Acta Crystallogr., Sect. A*, **32**, 239 (1976).

26) J. H. Ammeter, H. B. Bürgi, E. Gamp, V. Meyer-Sandrin, and W. P. Jensen, *Inorg. Chem.*, **18**, 733 (1979); K. Chandrasekhar and H. B. Bürgi, *Acta Crystallogr., Sect. B*, **40**, 387 (1976). M. Stebler and H. B. Bürgi, *J. Am. Chem. Soc.*, **109**, 1395 (1987).

27) C. P. Brock, W. B. Schweizer, and J. D. Dunitz, *J. Am. Chem. Soc.*, **107**, 6964 (1985).

28) Usually estimated in terms of the **T, L, S** model: V. Schomaker and K. N. Trueblood, *Acta Crystallogr., Sect. B*, **24**, 63 (1968).

29) C. K. Johnson in "Thermal Neutron Diffraction," ed by B. T. M. Willis, Oxford (1970), p. 132.

30) J. D. Dunitz and D. N. J. White, *Acta Crystallogr., Sect. A*, **29**, 93 (1973).

31) V. Schomaker and K. N. Trueblood, *Acta Crystallogr., Sect. A*, Supplement **40**, C-339 (1984).

32) For a vibrating particle in a quadratic potential, $V(x)=fx^2/2$, the classical Boltzmann distribution leads to an expression for the mean-square displacement, $\langle x^2\rangle=RT/f$. The possibilities, limitations, and dangers of using such mean-field potentials in the interpretation of atomic ADP's are discussed in the article mentioned in Ref. 22.

33) K. N. Trueblood and J. D. Dunitz, *Acta Crystallogr., Sect. B*, **39**, 120 (1983).

34) E. Maverick and J. D. Dunitz, *Mol. Phys.*, **62**, 451 (1987).

35) Standard deviations in U components attainable for heavier elements such as carbon are many times smaller than this.

36) P. Seiler, B. Martinoni, and J. D. Dunitz, *Nature (London)*, **309**, 435 (1984).

37) R. Bau, I. Brewer, M. Y. Chiang, S. Fujita, J. Hoffman, M. I. Watkins, and T. F. Koetzle, *Biochem. Biophys. Res. Commun.*, **115**, 1048 (1984).

38) P. Seiler and J. D. Dunitz, *Acta Crystallogr., Sect. B*, **35**, 1068 (1979).

39) P. Seiler and J. D. Dunitz, *Acta Crystallogr., Sect. B*, **35**, 2020 (1979).

40) The crystallographic R factor, sometimes called the agreement factor, sometimes the disagreement factor, is usually defined as $R=\sum|F_H(\text{obs})-F_H(\text{calc})|/\sum F_H(\text{obs})$.

41) The use of neutron diffraction to obtain the parameters describing the pro-molecule completely avoids the bias associated with the use of isolated-atom form factors. Difference densities obtained in this way are known as X—N densities. The main disadvantage, apart from the extra work and inconvenience, is that one has to contend with two sets of experimental error instead of one. For investigations where the electron density around hydrogen atoms is of special interest, e.g., in studies of hydrogen bonding, etc., the additional work and complications involved in the double experiment are certainly justified.

42) A useful account of the concepts and terms used in experimental charge density studies has been provided by P. Coppens, "Electron Distributions and the Chemical Bond," ed by P. Coppens and M. B. Hall, Plenum, New York (1982), p. 61.

43) J. D. Dunitz, W. B. Schweizer, and P. Seiler, *Helv. Chim. Acta*, **66**, 123 (1983).

44) For comparison, the highest peak in the total electron density amounts to about 40 e Å^{-3} (at the F atom).

45) L. Hirshfeld, *Acta Crystallogr., Sect. B*, **40**, 484 (1984).

46) The main difference is that the static density (Fig. 6A) shows two lobes of a p-orbital like density at the F atom, whereas this feature is absent in the vibrationally smeared density (Fig. 5). Related to this difference, the U component of the F atom in the p-orbital direction is larger in the refinement without deformation density terms. Because of the high correlation in the least-squares calculation between vibrational and deformation parameters, this difference is not particularly serious.

47) B. Delley, *Chem. Phys.*, **110**, 329 (1986).

48) F. L. Hirshfeld, *Acta Crystallogr., Sect. B*, **40**, 613 (1984).

49) J. M. Savariault and M. S. Lehmann, *J. Am. Chem.*

Soc., **102**, 1298 (1980).

50) J. D. Dunitz and P. Seiler, *J. Am. Chem. Soc.*, **105**, 7056 (1983).

51) K. Angermund, K. H. Klaus, R. Goddard, and C. Krüger, *Angew. Chem.*, **97**, 241 (1985); *Angew. Chem., Int. Ed. Engl.*, **24**, 237 (1985).

52) For a criticism of the conventional view, see M. A. Spackman and E. N. Maslen, *Acta Crystallogr., Sect. A*, **41**, 347 (1985).

53) The hydrogen molecule H_2 may not, after all, be a suitable prototype for the chemical bond in general; the H atom is atypical in that it lacks an inner core, and the molecule is atypical in that it contains only two electrons.

54) W. H. E. Schwarz, P. Valtazanos, and K. Ruedenberg, *Theor. Chim. Acta*, **68**, 471 (1985); W. H. E. Schwarz, L. Mensching, P. Valtazanos, and W. von Niessen, *Int. J. Quantum Chem.*, **29**, 909 (1986).

55) K. L. Kunze and M. B. Hall, *J. Am. Chem. Soc.*, **108**, 5122 (1986).

56) J. C. Slater, "Quantum Theory of Molecules and Solids," McGraw-Hill, New York (1965), Vol. 2, p. 113.

57) P. Seiler and J. D. Dunitz, *Helv. Chim. Acta*, **69**, 1107 (1986).

58) W. A. Harrison, "Electronic Structure and the Properties of Solids," Freeman, San Francisco (1980).